2015 International Symposium on Nonlinear Theory and its Applications
NOLTA2015, Kowloon, Hong Kong, China, December 1-4, 2015

Dependence of Noble Gas Absorption upon Crystal Orientation of Tungsten

Hiroaki Nakamura[†1,†2], Seiki Saito[‡], Atsushi M. Ito[†1] and Arimichi Takayama[†1]

†1 Department of Helical Plasma Research, National Institute for Fusion Science
322-6 Oroshi-cho, Toki, GIFU 509-5292, Japan
†2 Department of Energy Engineering and Science, Nagoya University
Furo-cho, Chikusa-ku, Nagoya 464-8603, Japan
‡Department of Electrical Engineering, National Institute of Technology, Kushiro College
2-32-1 Otanoshike-Nishi , Kushiro, Hokkaido, 084-0916, Japan
Email: hnakamura@nifs.ac.jp

Abstract—Tungsten nano structure, e.g. a bubble or a fuzz structure, has been studied recently by a lot of plasma-wall interaction researchers. The purpose of these researches is to avoid the decrease of the mechanical property and the heat conductivity of the original tungsten material. To achieve this purpose, we estimate the sputtering yield, the absorptivity and the mean depth of helium gas for the tungsten using BCA simulation code ACΨT (atomic collision in any structured target) We obtain the sputtering yield, the absorptivity and the mean depth of helium gases for the tungsten with crystal surfaces. We also found that these physical quantities depend on the crystal orientation of the target tungsten.

1. Introduction

Tungsten fuzz structure is one of the phenomena which attracts attention in the fusion science [1–4]. In our previous works, we showed the absorptivity as well as the penetration depth and sputtering yield which are basic information to reveal the fuzz formation of tungsten [5]. In these calculation, we used a binary collision approximation (BCA) to solve scattering phenomena between tungsten atoms and injected atoms, i.e., noble gas atoms. The BCA simulation is performed by ACΨT (atomic collision in any structured target) code [6–11]. In this paper, to focus on the target structure, we consider the crystal structure of tungsten whose surfaces are (100), (110) and (111). It is well-known that irradiated atoms can enter the crystal more deeply than the amorphous structure, because "channeling phenomena" occurs in the crystal [9]. Moreover, we treat the simplified fuzz structure in BCA simulation, to compare with crystals.

2. Simulation method

The algorithm of the simulation is the same as our previous papers [6–9]. Though carbon and hydrogen atoms are treated in our previous works, helium atom injection onto tungsten atoms is considered in the present work (see Fig. 1). In spite of the above difference, it is appropriate to employ the Moliere approximation [12] to the Thomas-Fermi

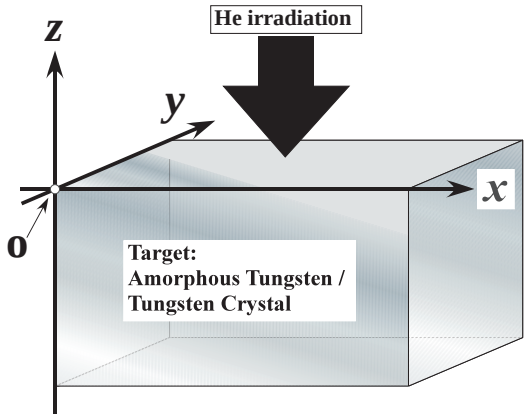

Figure 1: Schematic picture of He irradiation to tungsten targets: an amorphous structure and BCC crystals with (100), (110) and (111) surfaces. The *xyz* coordinate is adopted and the origin O is set in the surface of the tungsten. Periodic boundary conditions are used in the x- and the y-directions.

potential as the interatomic potential $V(r)$,

$$V(r) := \frac{Z_1 Z_2}{r}\phi\left(\frac{r}{a}\right), \quad (1)$$

$$a := \frac{0.4685}{\left(Z_1^{1/2}+Z_2^{1/2}\right)^{2/3}}, \quad (2)$$

$$\phi(x) := \sum_{i=1}^{3}\alpha_i e^{-\beta_i x}, \quad (3)$$

where r is the distance between the projectile and the target atoms (see Fig. 2). Z_1 and Z_2 are the atomic numbers of the projectile and target atom, respectively, and a is the screening length. Moreover, $\alpha_1 = 0.35$, $\alpha_2 = 0.55$, $\alpha_3 = 0.10$, $\beta_1 = 0.3$, $\beta_2 = 1.2$, $\beta_3 = 6.0$ are fitting parameters in Eq.(3) [10, 12].

The trajectories of projectile and target atoms are obtained using the scattering angle Θ in the center-of-mass system, which is related to the scattering angle θ_1 and the

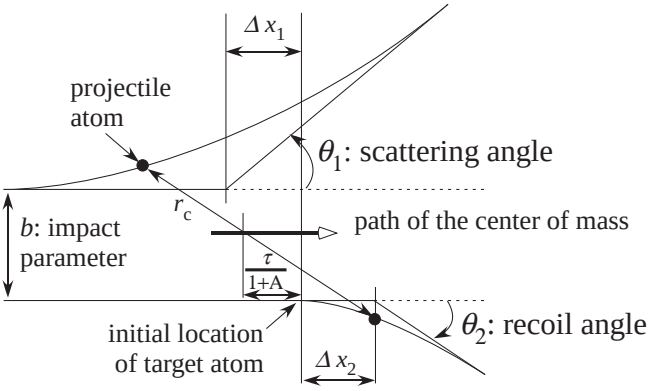

Figure 2: Schematic picture of two particles interaction with a conservative central repulsive force field $V(r)$ in the laboratory system [6,10]. The parameter A is the mass ratio of the projectile and the target, *i.e.*, m_2/m_1.

recoil angle θ_2 in the laboratory system in Fig. 2 as follows:

$$\tan\theta_1 = \frac{\sin\Theta}{\cos\Theta + \frac{m_1+m_2}{m_2}\frac{v_g}{v}}, \quad (4)$$

$$\tan\theta_2 = \tan\left(\frac{\pi}{2} - \frac{\Theta}{2}\right), \quad (5)$$

where v_g and v are the velocity of the center of mass and the relative velocity, respectively. Moreover, the scattering angle Θ is given as follows [6, 10].:

$$\Theta = \pi - 2b\int_{r_0}^{\infty}\frac{1}{r^2 g(r)}\mathrm{d}r, \quad (6)$$

where b is the impact parameter and

$$g(r) := \sqrt{1 - \frac{b^2}{r^2} - \frac{V(r)}{E_r}}, \quad (7)$$

$$E_r := \frac{m_1}{m_1+m_2}E_0. \quad (8)$$

Here m_1 and m_2 are the masses of the projectile ant target atoms, respectively. r_0 is the solution of $g(r_0) = 0$ and E_0 is the incident kinetic energy of the projectile.

In BCA simulation, the trajectories of the projectile and the target atoms are approximated as the asymptotes in the laboratory system [6, 10]. These trajectories consist of linked straight-line segments. The starting points Δx_1 and Δx_2 of the projectile and recoil atoms after the collision are given by

$$\Delta x_1 = \frac{2\tau + \left(\frac{m_2}{m_1} - 1\right) b\tan\left(\frac{\Theta}{2}\right)}{1 + \frac{m_2}{m_1}}, \quad (9)$$

$$\Delta x_2 = b\tan\left(\frac{\Theta}{2}\right) - \Delta x_1, \quad (10)$$

where

$$\tau := \sqrt{r_0^2 - b^2} - \int_{r_0}^{\infty}\left[\frac{1}{g(r)} - \frac{r}{\sqrt{r^2 - b^2}}\right]\mathrm{d}r. \quad (11)$$

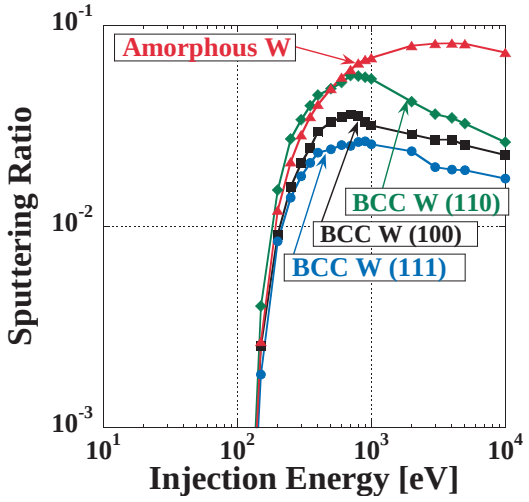

Figure 3: Sputtering ratio of He for tungsten targets, *i.e.*, amorphous structure and BCC crystals with (100), (110), (111) surfaces.

3. Simulation model

We adopted the four types, that is, BCC crystals with (100), (110) and (111) surfaces and an amorphous structure as the tungsten target, which is 15.825 Å long, 15.825 Å wide and 31650 Å deep, which consists of 5×10^5 tungsten atoms. Periodic boundary conditions are imposed on the horizontal direction. The lattice constant of tungsten is 3.165 Å. All tungsten atoms are fixed to the lattice points of BCC crystal without vibration, which means that the initial temperature of the tungsten is set to 0 K. $Z_1 = 2$ and $Z_2 = 74$ are adopted in Eqs. (1) and (2) as atomic numbers of He and W.

He atom whose the kinetic energy is in the range of 10 eV to 10^4 eV is injected vertically into the tungsten from its upper side (see Fig.1). W and He atoms are collided with each other, and then the final positions of all atoms, *i.e.*, W and Ar, are detected in each simulation. We repeated the above simulation $N_{\mathrm{sim}} = 2\times10^5$ times for each injection energy of He. The initial injection position of an He atom is changed randomly on each simulation.

4. Results

Using ACAT, sputtering yield Y, mean depth R and absorptivity A of He for each tungsten structure are calculated (see Figs. 3, 4 and 5).

The sputtering yield Y is obtained as follows. In $N_{\mathrm{sim}} = 2\times10^5$ simulations for the tungsten target, the number of tungsten atom released from the tungsten surface N_{W} was counted. The sputtering yield Y is given as $Y = N_{\mathrm{W}}/N_{\mathrm{sim}}$.

Next, the mean depth R is given by the following equation; $R = \sum_{i=1}^{N_{\mathrm{sim}}}|z_i^{\mathrm{f}}|/N_{\mathrm{sim}}$, where z_i^{f} is the $z-$coordinate of the final position of the irradiated He in the $i-$th simula-

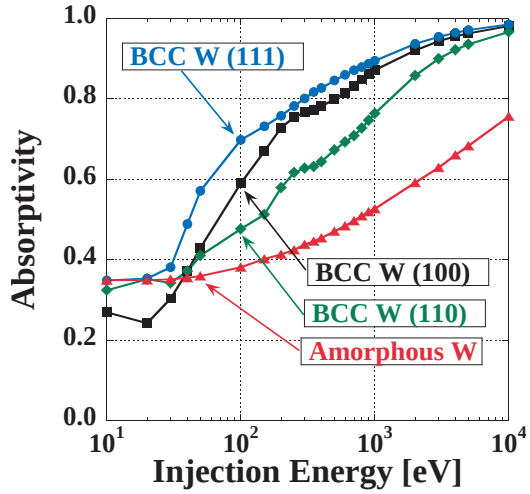

Figure 4: Absorptivity of He for tungsten targets, *i.e.*, amorphous structure and BCC crystals with (100), (110), (111) surfaces.

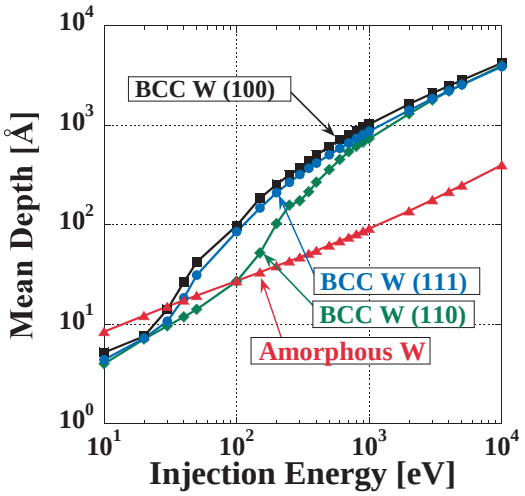

Figure 5: Mean depth of He for tungsten targets, *i.e.*, amorphous structure and BCC crystals with (100), (110), (111) surfaces.

tion. The $z = 0$ plane denotes the surface of the tungsten target as Fig. 1.

Concerning to the absorptivity A, the number of the He atoms whose $z_i^{\mathrm{f}} < 0$ is counted first (this number is defined as $N_{\mathrm{He}}^{\mathrm{a}}$). Using these quantities, the absorptivity A is given as $A = N_{\mathrm{He}}^{\mathrm{a}}/N_{\mathrm{sim}}$

For amorphous structure, the sputtering yield is largest in almost all of injection-energy region. However, the absorptivity and the mean depth is smallest in almost all of injection-energy region. Thus, it is found that amorphous structure is most fragile for He injection. Therefore it is concluded, from our BCA simulation, that amorphous structure is not adequate to the plasma facing material comparing with the other tungsten crystals. However, it is necessary to consider the other physical quantities, *i.e.*, melting point, thermal conductivity, to choose the plasma facing material.

Acknowledgments

This work was supported by JSPS KAKENHI Grant Number 15K06650 and the National Institute for Fusion Science (NIFS) Collaboration Research programs (NIFS14KNTS028, NIFS14KNTS043).

References

[1] H. Iwakiri, K. Yasunaga, K. Morishita, N. Yoshida: J. Nucl. Mater. **283–287** (2000) 1134.

[2] D. Nishijima, M.Y. Ye, N. Ohno, S. Takamura: J. Nucl. Mater. **329–333** (2004) 1024.

[3] S. Takamura, N. Ohno, D. Nishijima, S. Kajita: Plasma Fusion Res. **1** (2006) 051.

[4] S. Kajita, T. Saeki, Y. Hirahata, M. Yajima, N. Ohno, R. Yoshihara, N. Yoshida: Jpn. J. Appl. Phys. **50** (2011) 08JG01.

[5] H. Nakamura, S. Saito, A. M. Ito and A. Takayama: 6th International Symposium on Advanced Plasma Science and Its Applications for Nitrides and Nanomaterials/ 7th International Conference on Plasma-Nano Technology & Science (ISPlasma2014/ ICPLANCTS2014), Meijo University, Nagoya, Japan, March 2-6 (2014) 06aP06.

[6] A. Takayama, S. Saito, A.M. Ito, T. Kenmotsu and H. Nakamura: Jpn. J. Appl. Phys. **50** (2011) 01AB03.

[7] S. Saito, A. Takayama, A.M. Ito and H. Nakamura: Proceedings of the 31th JSST Anual Conference/ International Conference on Modeling and Simulation Technology (JSST2011), Tokai University, Tokyo, Japan, October 22-13 (2011) 251.

[8] S. Saito, A. Takayama, A.M. Ito, T. Kenmotsu and H. Nakamura: Progress in Nuclear Science and Technology, **2** (2011) 44.

[9] S. Saito, A. M. Ito, A. Takayama, and H. Nakamura: J. Nucl. Mat. Suppl. **438** (2013) S895.

[10] Y. Yamamura and Y. Mizuno: Inst. Plasma Phys., Nagoya University (1985) IPPJ-AM-40. (http://dpc.nifs.ac.jp/IPPJ-AM/IPPJ-AM-40.pdf)

[11] Y. Yamamura, I. Yamada and T. Takagi: Nucl. Instrum. Methods Phys. Res. Sect. B **37–38** (1989) 902.

[12] G. Mòliere: Z. Natureforsch. **A2** (1947) 133 [in German].